Low-Temperature Oxidation of di-n-Butyl Ether in a Motored Homogeneous Charge Compression Ignition (HCCI) Engine: Comparison of Characteristic Products with RCM and JSR Speciation by Orbitrap

Nesrine Belhadj, Zahraa Dbouk, Maxence Lailliau, Roland Benoit, Bruno Moreau, Fabrice Foucher, Philippe Dagaut

Low-Temperature Oxidation of di-*n*-Butyl Ether in a Motored Homogeneous Charge Compression Ignition (HCCI) Engine: Comparison of Characteristic Products with RCM and JSR Speciation by Orbitrap.

Nesrine Belhadj[a,b], Zahraa Dbouk[a], Maxence Lailliau[a,b], Roland Benoit[a], Bruno Moreau[b], Fabrice Foucher[b], Philippe Dagaut[a *]

[a]*Centre National de la Recherche Scientifique, INSIS, Institut de Combustion, Aérothermique, Réactivité, Environnement, 1C avenue de la recherche scientifique, 45071 Orléans, France*
[b]*Université d'Orléans, Laboratoire PRISME, 8 Rue Léonard de Vinci, 45100 Orléans, France*

*Corresponding author: Philippe Dagaut, Tel: +33 (0)2 38 25 54 66 - dagaut@cnrs-orleans.fr

ABSTRACT: Earlier, the oxidation of di-*n*-butyl-ether (DBE) carried out in a jet-stirred reactor (JSR) and in a rapid compression machine (RCM) revealed that it to proceeds similarly under both conditions (Belhadj et al, *Combust. Flame* **2020**, *222*, 133-144). Here, we extend that study to DBE oxidation in a motored homogeneous charge compression ignition engine, conditions under which this fuel has never been studied. Samples of exhaust gas were obtained by bubbling in acetonitrile maintained at 0°C. The samples were analyzed using atmospheric pressure chemical ionization in positive and negative modes, high-resolution mass spectrometry (Orbitrap), and ultra-high-pressure liquid chromatography. Flow injection analyzes of samples before and after H/D exchange using D_2O were also performed to verify the presence of isomeric products containing OH or OOH groups. Carbonyls were identified through derivatization with 2,4-dinitrophenyl hydrazine. A large set of chemical products of DBE cool flame were detected in the engine exhausts. They include hydroperoxides and diols ($C_8H_{18}O_3$), unsaturated diols or unsaturated hydroperoxides ($C_8H_{16}O_3$), ketohydroperoxides ($C_4H_8O_3$ and $C_8H_{16}O_4$), di-keto ethers ($C_8H_{14}O_3$), olefinic di-keto ethers ($C_8H_{12}O_3$), cyclic and keto-ethers ($C_8H_{16}O_2$), olefinic cyclic and keto-ethers ($C_8H_{14}O_2$). Also, highly oxygenated chemicals, i.e., keto-dihydroperoxides ($C_8H_{16}O_6$) resulting from three O_2 additions on radicals from the fuel, diketo-hydroperoxides ($C_8H_{14}O_5$) resulting from decomposition of keto-dihydroperoxides ($C_8H_{16}O_6$), addition to other oxygenated intermediates i.e., hydroxy-DBE ($C_8H_{18}O_2$) and organic peroxides ROOR' ($C_{16}H_{34}O_4$, $C_{11}H_{24}O_3$, $C_{11}H_{22}O_3$, and $C_{10}H_{22}O_3$), were observed in the engine exhausts. The present speciation results of the engine exhausts were compared to those obtained for samples of the oxidation of DBE in an RCM and a JSR. Despite the significant differences in physical experimental conditions, the present study indicates a common oxidation mechanism proceeds in JSR, RCM, and motored engine, leading to the formation of products having the same chemical formulas and retention times.

Keywords: biofuel; cool flame; jet-stirred reactor; rapid compression machine; motored engine; UHPLC; mass spectrometry; Orbitrap

1. INTRODUCTION

Several previous investigations of products formed in piston and motored engines have been published in the mid-1980s-1990s, following pioneer investigations, e.g., [1]. Most of them concern the oxidation of hydrocarbons and the formation of stable products, e.g., olefins, aldehydes, and cyclic ethers [2-4].

In the late 1990s, less stable oxidation products have been measured, e.g., hydroperoxides, ketohydroperoxides, and polycarbonyl-hydro-peroxides [5-7]. Several analytical techniques were used in these studies, i.e., gas chromatography and detection by flame ionization (GC-FID) [1-4] and mass spectrometry (GC-MS) [5-7], and high-pressure liquid chromatography coupled to mass spectrometry and UV detection [5]. The authors reported the formation of alkylhydroperoxides [5], ketohydroperoxides [6], and poly-ketohydroperoxides [7].

In the mid-2000s, Wang et al. [8] studied the formation of cool flame intermediates from *n*-heptane oxidation in a jet-stirred reactor (JSR) and a cooperative fuel research (CFR) engine. Products formed in JSR were analyzed using synchrotron vacuum ultraviolet radiation photoionization time-of flight molecular-beam mass spectrometry (SVUV-PI-MBMS). CFR exhausts were analyzed using a high-resolution mass spectrometer (HRMS) with atmospheric pressure chemical ionization (APCI). Products of third O_2 addition of radicals from the fuel were detected. Their results showed good agreement between intermediate species, in terms of chemical formulae, detected in JSR and CFR experiments. In several studies, speciation of oxidation products and intermediates formed during the combustion of biofuels under motored engines conditions have been reported. Szybist et al. [9] studied the combustion of *n*-heptane, methyl decanoate and diesel fuels in a motored engine. Fourier transform infrared (FTIR) spectrometry and gas chromatography coupled to mass spectrometry (GC/MS) were used for speciation. Among the products of oxidation, the authors reported the formation of diones which can derive from ketohydroperoxides (KHP) decomposition. Boehman and co-workers [10-12] explored the low to intermediate temperature oxidation of a series of biodiesel surrogates (cyclohexane, methyl cyclohexane, methyl heptanoate and ethyl hexanoate, 1-butanol, and mixture of *n*-heptane/1-butanol) and *n*-heptane primary reference fuel in a modified CFR engine operated with compression ratios of 4.43 to 15. Exhaust gases were collected in the gas phase and liquid phase. Liquid samples have been collected by bubbling exhaust gas into dichloromethane maintained at -73°C using a dry ice/acetone bath. These samples were analyzed by GC-MS. Gases not trapped in dichloromethane were collected at the exit of the bubbler and analyzed using a GC with flame ionization and thermal conductivity detectors (FID, TCD). Exhaust gases without using the cold bath were analyzed similarly. Liu et al.[13] studied the effect of inlet pressure and octane numbers on emissions of an homogeneous charge compression ignition (HCCI) engine. They showed that unburnt hydrocarbons, CO, and NOx emissions decrease using supercharging. That study also showed that the emissions of unburnt hydrocarbons and CO when

burning gasoline are higher than those measured using PRF with supercharging. An extensive literature review published in 2019 give an overview of current knowledge on HCCI emissions[14].

More recently, Al-Gharibeh et al. [15-16] have investigated the low-to-intermediate temperature oxidation of *n*-heptane and methyl decanoate in a motored engine at compression ratios of 5 to 7.75 and 5.5 to 9, respectively. An oil-free metal bellows vacuum pump was used to draw gaseous exhaust in their experiments. FTIR and GC-MS were used to identify stable species (CO, CO_2, alkenes, ketones, aldehydes, ethers, alcohols, etc.).

Recently, Belhadj et al.[17] performed a characterization of the cool flame products of *n*-heptane-isooctane 50/50 mixture in a JSR, a RCM and a motored HCCI engine. They collected exhaust gases through bubbling in cooled acetonitrile and analyzed the resulting solutions by ultra-high-pressure liquid chromatography (UHPLC) coupled to high-resolution mass spectrometry (HRMS Orbitrap Q-Exactive™). Cool flame products were characterized by tandem mass spectrometry, H/D exchange using D_2O, and 2,4-dinitrophenylhydrazine derivatization of carbonyl products. In addition to aldehydes, cyclic ethers, and ketones ($C_7H_{14}O$, $C_8H_{16}O$), ketohydroperoxides ($C_7H_{14}O_3$, $C_8H_{16}O_3$), diketones ($C_7H_{12}O_2$, $C_8H_{14}O_2$), and keto-dihydroperoxides ($C_7H_{14}O_5$, $C_8H_{16}O_5$) detected earlier[18], other low-temperature oxidation products were reported (hydroperoxides, diols, olefinic hydroperoxides, olefinic diols, dihydroperoxides, olefinic dihydroperoxides, olefinic cyclic ethers, olefinic carbonyls, di- and tri-olefinic cyclic ethers, ketones, or aldehydes, olefinic ketohydroperoxides, di-olefinic ketohydroperoxides, triketones, olefinic diketones, di-olefinic diketones, and diketo-hydroperoxides. Their results indicated strong similarities in terms of products detected in the three experiments. Again, the above mentioned studies mainly concern the oxidation of alkanes and primary reference fuels. To date, no similar studies have been performed for promising biofuels such as di-*n*-butyl ether. Then, as mentioned earlier[19], it would be interesting to study the oxygenated molecules formed during the oxidation of di-*n*-butyl ether in a motored engine. This would complement the existing body of information acquired using laboratory experiments (JSR, rapid compression machine).

The aim of this paper is to provide new speciation data for the low temperature oxidation of di-*n*-butyl ether using a motored engine and compare them with those obtained using a JSR and an RCM for probing the existence of common oxidation routes and products. To this end, motored engine experiments were performed using a modified HCCI engine type DW10. Products were sampled by bubbling a fraction of the engine exhausts in cooled acetonitrile. The samples were analyzed by flow injection (FIA) and ultra-high-pressure liquid chromatography coupled to a high-resolution mass spectrometer (UHPLC-HRMS).

2. EXPERIMENTS

In the present work, the formation of intermediate oxygenated molecules during the low-temperature oxidation of di-*n*-butyl ether (>99 % pure, from Sigma Aldrich®) was investigated using a HCCI motored engine (Table 1).

Table 1. Homogeneous charge compression ignition specifications and operating conditions.

Description (units)	Value
Bore (mm)	85
Stroke (mm)	88
Connecting rod (mm)	145
Geometric compression ratio (-)	9.2
Number of Valves	4
Intake Valve Closure (CAD)	351
Intake Valve Opening (CAD)	157
Exhaust Valve Opening (CAD)	140
Exhaust Valve Closure (CAD)	366
Engine speed (r/min)	1500
Coolant temperature (°C)	90
Oil temperature (°C)	90
Intake manifold pressure (kPa)	95
Global equivalence ratio (-)	0.5
Oxygen concentration (%)	12
Volume of gas sampled (L)	100

Table 2. JSR and RCM experimental conditions.

	JSR	RCM
Reactive mixture	0.5% DBE, 12% O_2, 87.5% N_2	DBE/air (21% O_2, 79% N_2)
Equivalence ratio (φ)	0.5	0.5
	Residence time: 1 s	Compression time: <4 ms
Pressure (bar)	10	5
Temperature (K)	480-670	550-630
Volume of gas sampled (L)	45	0.5

Because we are comparing the present speciation with those deriving from previous experiments,[19] the experimental conditions for the oxidation of DBE in RCM and JSR are summarized in Table 2. The JSR and rapid compression machine experimental setups have already been described in detail previously[18-21].

2.1 Motored engine setup. The engine used here is a single-cylinder conventional Diesel engine (DW10 from PSA®), modified to run in HCCI mode and coupled to an electric motor to maintain a constant rotation speed. The piston from the conventional engine was used and the compression ratio was decrease to 9.2:1 by adjust the distance between the piston and the cylinder head. The main characteristics of this engine are given in Table 1. In the present study, in order to control ignition, air was diluted by nitrogen to decrease the oxygen concentration down to 12% and the equivalence ratio

was set to 0.5. Each flow of gases and liquids was controlled by mass flow controllers (Emerson® CMFS025M for air, Brooks® 5835S for nitrogen, and Bronkhorst® M13 Mini Coriflow for DBE) and introduced inside a plenum upstream of the combustion chamber to prepare a perfectly homogeneous mixture. DBE was injected into the plenum after an initial dilution with air and a preheating allowing its evaporation. An electric resistor was used to maintain a constant temperature (300 K) close to the intake valves. Air and nitrogen flows came from an air compressor and a nitrogen generator, respectively. They were dried at a -40°C dew point to avoid ice formation during the sampling. Intake pressure was regulated at 0.95 bar to maintain the cool flame close to the top dead center and to quench the main flame during the expansion stroke. Intake temperature was measured with two K-type thermocouples, one in each intake port, with an accuracy of ± 2 K, and was controlled by a main heater warming up the main air flow and a band heater set around the plenum. In-cylinder pressure was measured by a Kistler 6043A piezo-electric sensor with an accuracy of ±2%, intake pressure was measured by a Kistler 4075A piezoresistive absolute pressure sensor, with an accuracy of ±0.3% of the full scale. For all the experiments, intake and in-cylinder pressures were recorded with a resolution of 0.1 CAD using a Külber 8.5020.D842.3600 encoder set on the crankshaft and data were analyzed over 100 consecutive cycles. A schematic representation of the experimental setup is shown in Figure 1.

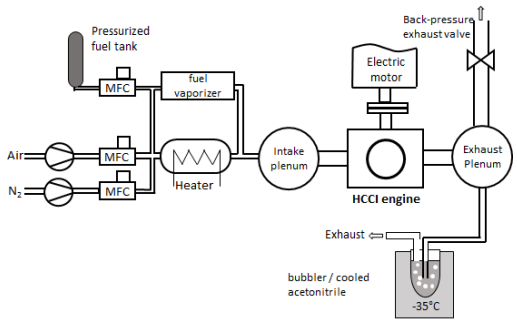

Figure 1. Schematic of the HCCI motored engine setup. The acetonitrile trapping system from the exhaust plenum is presented.

Typical recordings of in-cylinder pressure, temperature, and heat release rate as a function of crank angle are presented in Figure 2. From that figure, one can see that the pressure in the cylinder reached a maximum of 15 bar and the temperature increased to 780 K. A weak low-temperature heat release rate of 4 J/CAD, similar to that measured in previous motored engine experiments [8], was also recorded. Under the present operating conditions, the main ignition yielding high-temperature heat release is avoided, which allows probing low-temperature oxidation products under engine relevant conditions.

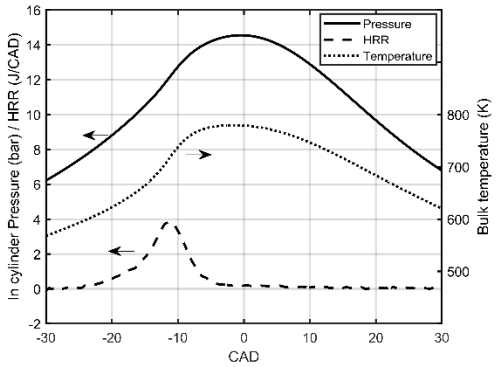

Figure 2. In-cylinder heat release rate (HRR) and pressure (left y-axis) and temperature (right y-axis) recorded as a function of crank angle degree (CAD).

Engine exhaust sampling was performed using a midget bubbler (Supelco®) filled with 15 mL of cooled acetonitrile (ACN) and immersed in a paraffin oil bath maintained at -35°C. Bubbling lasted 20 min. Back pressure was regulated at 1.05 bar to allow exhaust gas flow through the bubbler. The exhaust gas flow through the bubbler was fixed to 200 Nl/h.

2.2 Chemical analyzes. Exhaust chemical species dissolved in ACN were analyzed by reversed phase ultra-high-pressure liquid chromatography (RP-UHPLC) using a C_{18} column (1.6 µm, 100 Å, 2.1 mm, 100 mm, Luna Omega from Phenomenex®) under the following elution conditions: mobile phase (H_2O+ACN), 5 to 90% of ACN; flow rate of 250 µl/min during 20 min. Additional flow injection analyzes (FIA) were performed as well as isotopic H/D exchange tests using D_2O (Sigma-Aldrich®) for probing the presence of OH and OOH groups in products, as employed previously[17-19, 22-23], 300 µl of D_2O were introduced into 1 ml of DBE oxidation sample (reaction time 20 min at 20°C). H/D exchange occurs only with labile hydrogen sites whereas for non-exchangeable hydrogen atoms like those in C-H groups, H/D exchange requires catalysis[24]. The carbonyl functions were characterized by 2,4-dinitrophenylhydrazine (DNPH, from Sigma-Aldrich®) derivatization: 2,4-DNPH ($C_6H_6O_4N_4$) + carbonyl species → dinitrophenylhydrazones + H_2O. To this end, 50 µl of saturated DNPH solution in acetonitrile were added to samples. As in previous works [19, 22, 25-26], atmospheric pressure chemical ionization (APCI in positive mode, $[M+H]^+$, and negative mode, $[M–H]^–$) coupled to an Orbitrap Q-Exactive™ high resolution mass spectrometer (resolution of 140,000; mass accuracy < 1 ppm at *m/z* 200) from Thermo Fisher Scientific® was used to detect oxidation products in samples. In order to identify low-temperature products, MS/MS analysis were performed at collision cell energy of 10 eV.

3. RESULTS AND DISCUSSION

Cool flame oxidation products of di-*n*-butyl ether in the engine exhausts were detected by UHPLC/HRMS. The present experimental results and those obtained in a JSR and a RCM, and partially published previously[19] were compared. Unsaturated hydroperoxides or unsaturated diols ($C_8H_{16}O_3$), light keto-hydroperoxides ($C_4H_8O_3$), olefinic cyclic ethers and olefinic carbonyl ($C_8H_{14}O_2$), olefinic diones ($C_8H_{12}O_3$), hydroxy-DBE ($C_8H_{18}O_2$), diketohydroperoxides ($C_8H_{14}O_5$), and organic peroxides

(ROOR') were not reported in our previous publication [19]. In this section we present the results of our new measurements and compare them to the data resulting from previous oxidation experiments in a JSR and an RCM.

3.1 Formation of diols, hydroperoxides ($C_8H_{18}O_3$), and unsaturated diols or hydroperoxides ($C_8H_{16}O_3$). Diols, hydroperoxides ($C_8H_{18}O_3$), and unsaturated diols or hydroperoxides ($C_8H_{16}O_3$) can be formed during DBE low-temperature oxidation [19]. Analyses using RP-UHPLC coupled to HRMS (APCI+) revealed the presence of $C_8H_{18}O_3$ isomers in JSR samples. They could not be detected in RCM samples due to higher dilution. However, we could detect them in samples from motored engine exhaust, as shown in Figure 3.

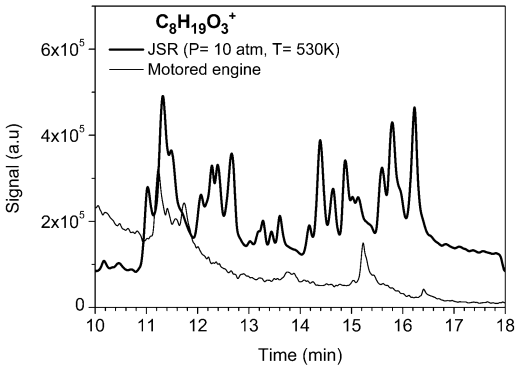

Figure 3. $C_8H_{18}O_3$ formation during the cool flame oxidation of DBE in JSR and motored engine. Signals are obtained using positive APCI ($C_8H_{19}O_3^+$, *m/z* 163.1325).

There, it can be seen that the formation of $C_8H_{18}O_3$ isomers is more evident in samples from JSR experiments than from motored engine experiments. Hydroperoxides formation can result from H-atom abstraction by peroxy radicals, i.e., $ROO^{\bullet} + R'H \rightarrow ROOH + R'^{\bullet}$ and $ROO^{\bullet} + HOO^{\bullet} \rightarrow ROOH + O_2$. These species are relatively unstable, which could explain lower concentrations in engine samples where they could decompose on metallic surfaces. Diols with the same chemical formula could be formed through the decomposition of dihydroperoxides [27]. Their formation has been reported earlier in JSR experiments [19] on the basis of double H/D exchange using D_2O. Here, in engine samples, diols seem to be present in chromatographic peaks at $11 < t/min < 12$ and t= 15.3 min, as reported earlier [19]. The engine data seem to indicate that diols are the main isomers present whereas ROOH, more prone to decomposition on metallic surface, are most likely present at trace levels. To further assess the presence of diols, we performed H/D exchange using D_2O. No deuterated products were detected without addition of D_2O to the samples. The analyzes of samples containing D_2O showed one and two H/D exchanges, which could correspond to ROOH and diols, respectively (Table 3). These findings are in line with previous results obtained with samples from DBE oxidation in a JSR [19]. MS/MS analysis of $C_8H_{19}O_3^+$ (m/z 163.1325) revealed the presence of several fragments proving the presence of hydroperoxides and diols in DBE oxidation samples. For example, $C_4H_9O_2^+$ (m/z 89.0595), $C_2H_5O_2^+$ (m/z 61.0284), and $C_4H_9^+$ (57.0698) fragments are common to both hydroperoxides and diols, but the $C_3H_7O^+$ fragment

(m/z 59.0492) is characteristic of diols. MS/MS spectra and identification of fragments are shown in the Supporting Information 1.

Table 3. Analysis by FIA-APCI (+/–)/HRMS of engine exhaust gases after H/D exchange.

Ion, *m/z*	Signal (a.u.)
$C_8H_{19}O_3^+$, 163.1325	$2.99x10^6$
$C_8H_{18}D_1O_3^+$, 164.1385	$3.27x10^6$
$C_8H_{17}D_2O_3^+$, 165.1447	$1.18x10^6$
$C_8H_{17}O_3^+$, 161.1170	$2.98x10^7$
$C_8H_{16}D_1O_3^+$, 162.1226	$2.39x10^7$
$C_8H_{15}D_2O_3^+$, 163.1290	$5.42x10^6$
$C_8H_{15}O_6^-$, 207.0874	$3.38x10^6$
$C_8H_{14}D_1O_6^-$, 208.0938	$5.92x10^6$
$C_8H_{13}D_2O_6^-$, 209.0999	$1.79x10^6$
$C_8H_{13}O_5^-$, 189.0769	$3.26x10^7$
$C_8H_{12}D_1O_5^-$, 190.0833	$2.28x10^7$
$C_8H_{19}O_2^+$, 147.1374	$4.88x10^6$
$C_8H_{18}D_1O_2^+$, 148.1437	$4.60x10^6$

Analyses performed using C_{18}-UHPLC/HRMS allowed detecting $C_8H_{16}O_3$ isomers (positive APCI, $C_8H_{17}O_3^+$, *m/z* 161.1170) corresponding to unsaturated diols and unsaturated hydroperoxides (Figure 4). H/D exchange was used to verify the presence of unsaturated ROOH and unsaturated diols. The results are presented in Table 3. They indicate the presence of unsaturated diols ($C_8H_{15}D_2O_3^+$) whereas $C_8H_{16}D_1O_3^+$ could be formed by both ROOH and diols. Proposed formation routes for unsaturated hydroperoxides are given in Scheme 1 (a-e).

In Figure 4, we compare chromatograms obtained for JSR, RCM, and engine samples. One can see that most of the $C_8H_{16}O_3$ isomers are observed in both JSR and engine sample (Figure 4a). The data obtained for JSR samples are also in line with those obtained for RCM and engine samples (Figure 4b). Despite an imperfect match of the 3 chromatograms obtained for $C_8H_{16}O_3$ isomers, one can conclude that rather similar products were formed under the 3 conditions considered here.

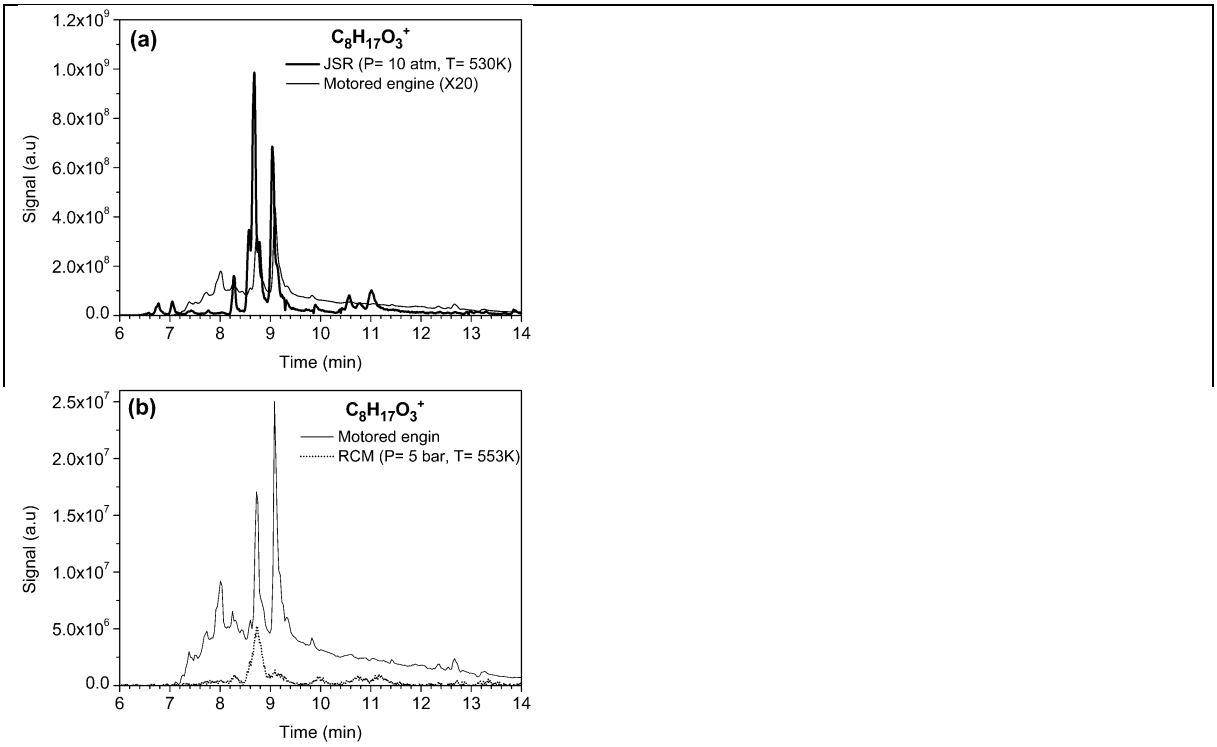

Figure 4. $C_8H_{16}O_3$ formation during the low-temperature oxidation of DBE in (a) JSR compared to motored engine conditions, and (b) RCM compared to motored engine conditions. The chromatogram from the motor engine sample analysis was multiplied by a factor of 20 (Figure 4a).

Scheme 1. Proposed formation routes for $C_8H_{16}O_3$ unsaturated hydroperoxides.

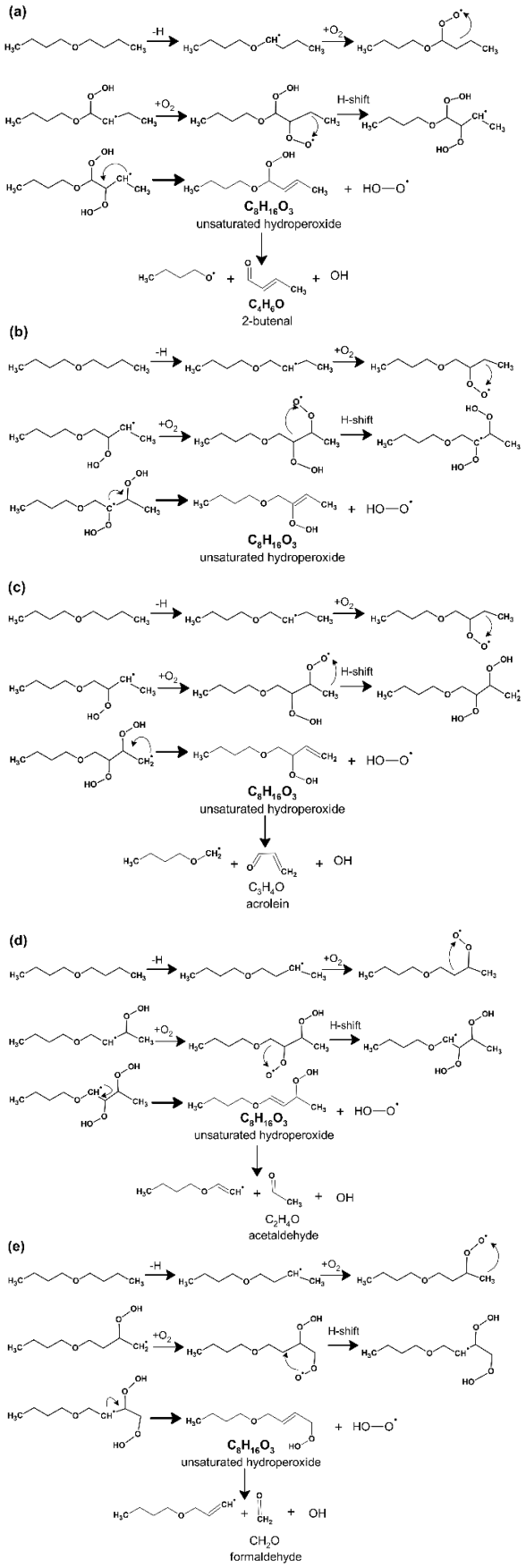

3.2 Formation of $C_8H_{16}O_4$ and $C_4H_8O_3$ ketohydroperoxides. $C_8H_{16}O_4$ and $C_4H_8O_3$ ketohydroperoxides (KHPs) are formed during the low-temperature oxidation of di-*n*-butyl ether [19, 28]. $C_8H_{16}O_4$ keto-hydroperoxides are formed through the following well-accepted combustion chemistry reactions pathways: DBE + X$^{\bullet}$ ($^{\bullet}$OH, H$^{\bullet}$, O$^{\bullet}$, $HO_2^{\bullet}$, O_2…) → R$^{\bullet}$ + XH; R$^{\bullet}$ + O_2 → ROO$^{\bullet}$ → $^{\bullet}$QOOH (H-shift); $^{\bullet}$QOOH + O_2 → $^{\bullet}$OOQOOH → HOOQ'=O + $^{\bullet}$OH. Concerning $C_4H_8O_3$ ketohydroperoxides, their production can occur through the following sequence of reactions: fuel + X$^{\bullet}$ → R$^{\bullet}$ + XH; R$^{\bullet}$ + O_2 → ROO$^{\bullet}$ → $^{\bullet}$QOOH (H-shift) → decomposition of $^{\bullet}$QOOH → carbonyl compound + R'OO$^{\bullet}$ → $^{\bullet}$Q'OOH (H-shift), $^{\bullet}$Q'OOH + O_2 → $^{\bullet}$OOQ'OOH → HOOQ''=O + $^{\bullet}$OH. The reaction pathway to $C_4H_8O_3$ is presented in Scheme 2.

Scheme 2. Proposed formation route for $C_4H_8O_3$ ketohydroperoxides.

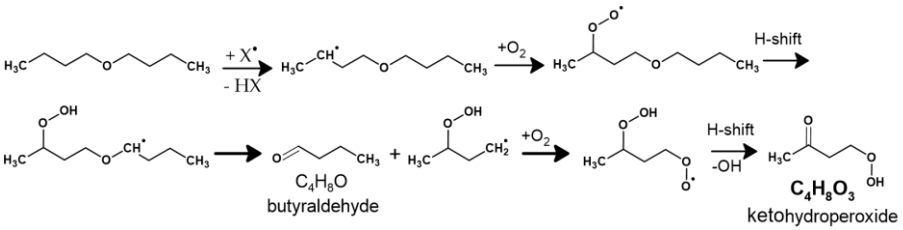

The use of RP-UHPLC coupled to HRMS (APCI+) allowed us to detect $C_8H_{16}O_4$ and $C_4H_8O_3$ KHPs as $C_8H_{17}O_4^+$ ions with *m/z* 177.1121 and $C_4H_9O_3^+$ ions with *m/z* 105.0543 in samples taken from a JSR and an RCM [19], and in samples obtained from the present motored engine experiments. Results are shown in Figure 5a-d. From that figure, one can observe similarities between JSR, RCM, and motored engine experimental datasets. However, it is noticeable that we obtained stronger signals for KHPs isomers in the case of JSR samples than in RCM and motored engine samples. Nevertheless, according to our chromatographic analyses, most of the KHPs isomers are formed in the three experimental setups, despite their different physical conditions. However, a closer look at the data indicated that some KHPs isomers could not detected in motored engine and RCM samples, i.e., $C_8H_{16}O_4$ isomers with retention times (R_t) ranging from 12 to 13.5 min. This could be due to higher chemical instability of these isomers. For KHPs with C=O and OOH groups on adjacent carbon atoms, hydrogen bonding (C-O....HOO) can provide higher stability to these isomers compared to those with more distant C=O and OOH groups for which intramolecular hydrogen bonding cannot occur. Still, KHPs decomposition is expected to be favored in presence of hot metallic surfaces, e.g., engine piston chamber and exhaust pipe. C_8-KHP and C_4-KHP detection was confirmed via 2,4-DNPH derivatization, but no standard could be used for confirming their chemical structure (Supporting information, Table S1).

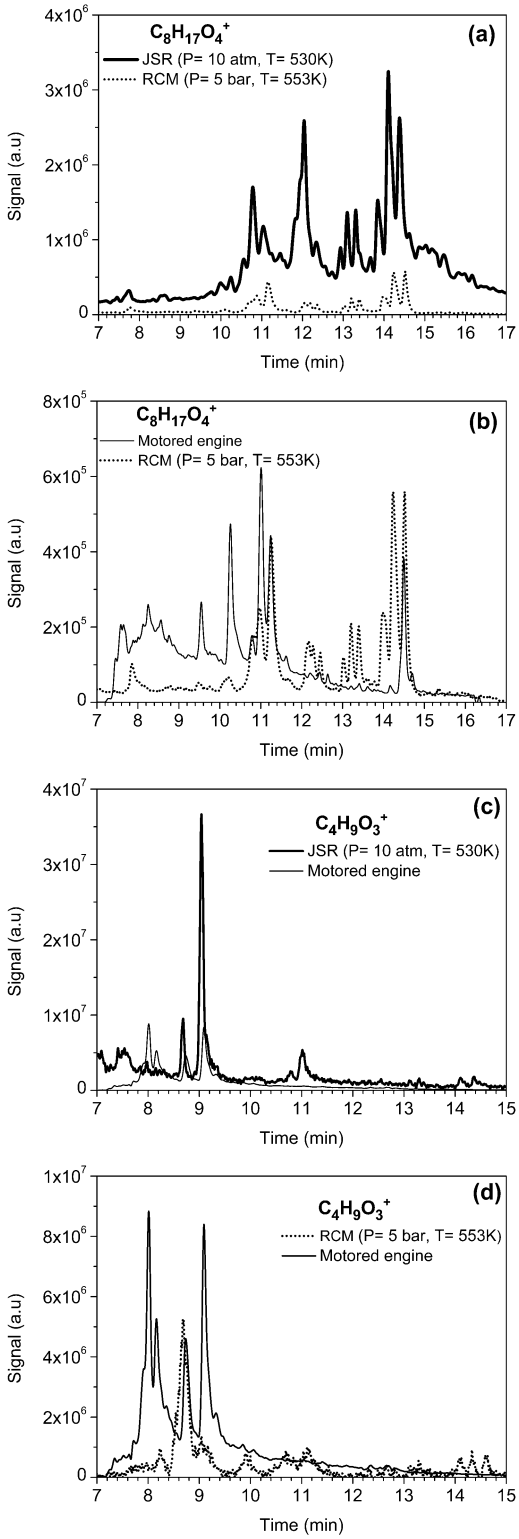

Figure 5. UHPLC-HRMS (APCI+) analyses results showing (a, b) C_8 and (c, d) C_4 ketohydroperoxides ($C_8H_{17}O_4^+$, *m/z* 177.1121 and $C_4H_9O_3^+$, *m/z* 105.0543) formed during DBE oxidation.

3.3 Formation of cyclic ethers and keto-ethers ($C_8H_{16}O_2$), and olefinic cyclic ethers and keto-ethers ($C_8H_{14}O_2$). Decomposition of DBE's $^{\bullet}$QOOH radicals can produce cyclic ethers ($^{\bullet}$QOOH → cyclic ethers + $^{\bullet}$OH) [28-30]. The chemical formula of cyclic ethers, $C_8H_{16}O_2$, is also that of keto-ethers such as butoxy-butanones, and esters, i.e., butyl butyrate, which can be formed from recombination of

DBE-yl-hydroperoxy radical ($C_8H_{17}O_3^{\bullet}$) or H-atom abstraction on ROOH followed by decomposition ROOH + $X^{\bullet}$ → HX + $R_{(-H)}$=O + $^{\bullet}$OH [29]. Figure 6 presents chromatograms obtained for the $C_8H_{17}O_2^+$ ion (*m/z* 145.1222 using APCI+) under JSR, RCM, and motored engine conditions. From that figure, one can see that all the data match well. Nevertheless, as noticed for other products detected in the present study, because the RCM samples were less concentrated than the JSR and motored engine samples, a weaker signal was recorded (Figure 6b). As demonstrated in our previous work[28], butyl butyrate was identified at R_t = 14.85 min using UHPLC. However, the non-availability of butoxy-butanones and cyclic ethers, i.e., lactones, made their identification difficult. The only way to distinguish them was using 2,4-DNPH derivatization. Results indicated that butoxy carbonyls have retention times in the range 11.10 to 11.65 min, and other peaks correspond to cyclic ethers[28].

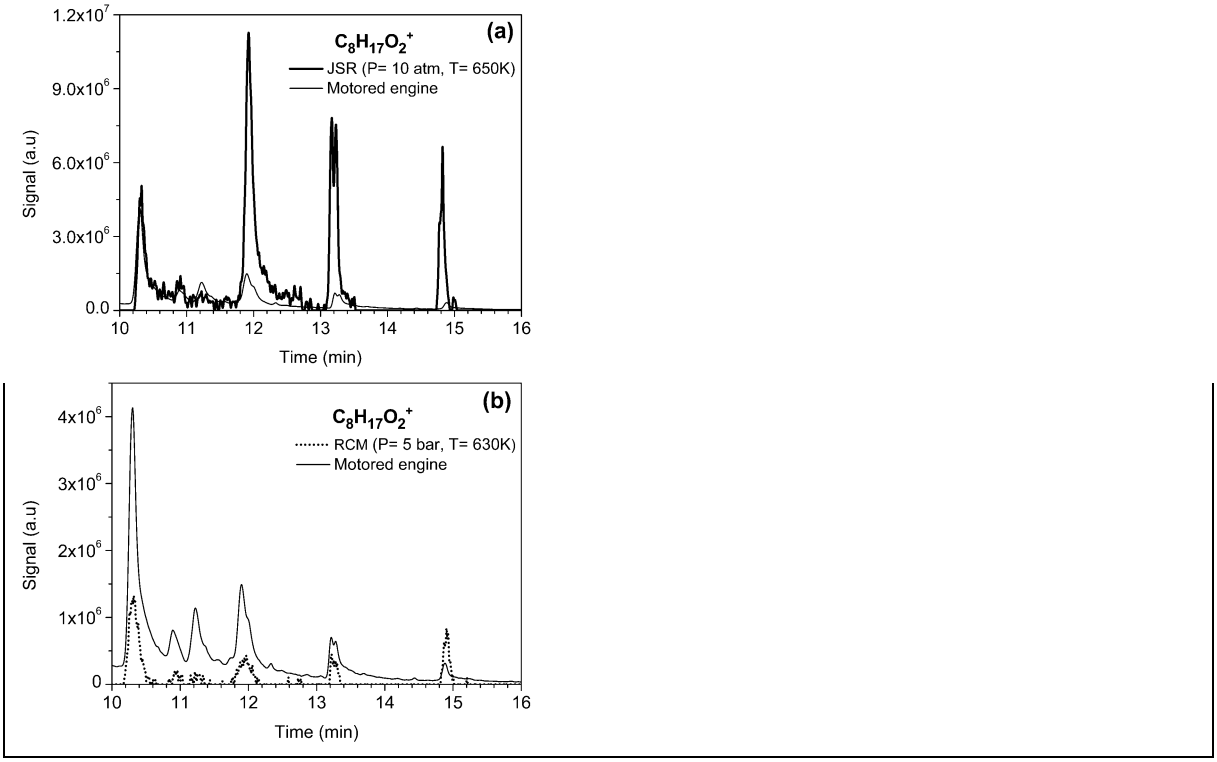

Figure 6. Comparison between UHPLC-HRMS(APCI+) signal for $C_8H_{17}O_2^+$ (*m/z* 145.1222) corresponding to cyclic ethers and keto-ethers isomers produced in (a) JSR and motored engine and (b) RCM and motored engine conditions.

The oxidation of $C_8H_{16}O_2$ (cyclic ethers and keto-ethers) can form olefinic cyclic ethers and olefinic keto-ethers ($C_8H_{14}O_2$): QO + $X^{\bullet}$ ($^{\bullet}$OH, $HO_2^{\bullet}$, $H^{\bullet}$, $O^{\bullet}$ …) → $Q^{\bullet}O$ + XH; $Q^{\bullet}O$ + O_2 → $^{\bullet}$OOQO → HOO$Q^{\bullet}O$ (H-shift) → $Q^{'}O$ + $HO_2^{\bullet}$. UHPLC-APCI(+)-HRMS analyses of JSR, RCM, and motored engine samples revealed the several $C_8H_{15}O_2^+$ isomers (*m/z* 143.1065) are present, as shown in Figure 7. Despite the weak signal of the RCM sample, we observed very similar chromatograms. The $C_8H_{15}O_2^+$ signal is more important for the motored engine sample (motored HCCI> JSR> RCM).

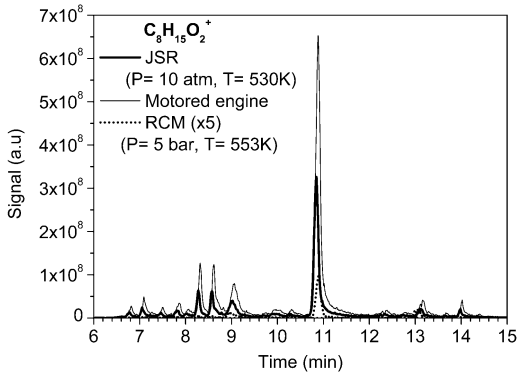

Figure 7. Chromatograms obtained in C_{18}-UHPLC/HRMS analysis of $C_8H_{15}O_2^+$ (*m/z* 143.1065) formed under JSR, motored engine, and RCM conditions.

The distinction between olefinic cyclic ethers and olefinic carbonyls was obtained using DNPH derivatization. The comparison of the $C_8H_{15}O_2^+$ signal before and after derivatization, allowed us to identify olefinic cyclic ethers isomers which did not react with DNPH ($ symbol). As can be seen in Figure 8, there are more DBE- olefinic carbonyls (# symbol) than DBE-olefinic cyclic ethers ($ symbol).

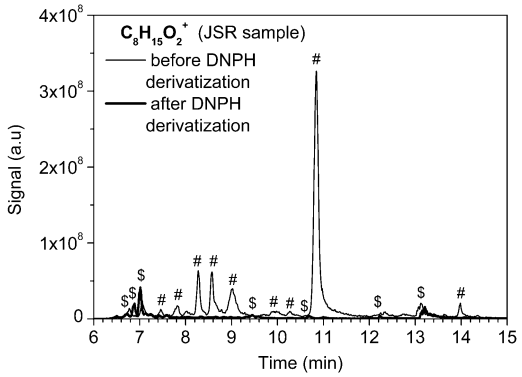

Figure 8. Comparison of chromatograms obtained by C_{18}-UHPLC/HRMS analyses of $C_8H_{15}O_2^+$ (*m/z* 143.1065) before and after DNPH derivatization. $ indicates DBE-olefinic cyclic ethers and # indicates DBE- olefinic carbonyls. JSR (530 K) sample results are shown.

3.4 Formation of diketo-ethers ($C_8H_{14}O_3$) and olefinic diketo-ethers ($C_8H_{12}O_3$). Diketo-ethers ($C_8H_{14}O_3$) can be produced by decomposition of KHPs isomers [7, 19, 31]. C_{18}-UHPLC-HRMS (APCI+) analyses revealed the presence of several $C_8H_{14}O_3$ isomers ($C_8H_{15}O_3^+$, *m/z* 159.1015). Our previous work[28] indicated that butyric anhydride was identified at R_t = 7.18 min. Figure 9 shows that butyric acid is not predominant. As can be seen from Figure 9, the production of $C_8H_{14}O_3$ isomers is similar under JSR and RCM conditions. We observed higher production of $C_8H_{14}O_3$ species under motored engine conditions. This could be due to more important depletion of KHPs forming diketo-ethers, i.e., HOOQ=O + X$^\bullet$ → O=Q'=O + XH + $^\bullet$OH, under motored engine conditions.

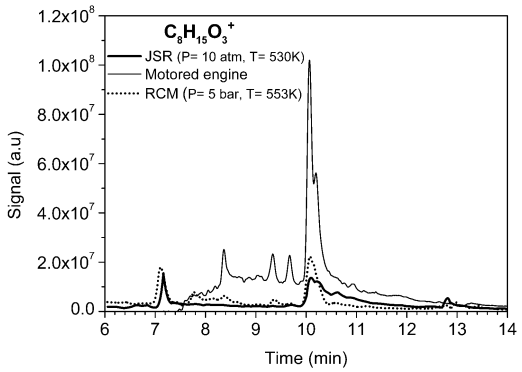

Figure 9. C_{18}-UHPLC/HRMS showing $C_8H_{14}O_3$ diketo-ethers isomers produced during cool flame oxidation of DBE under JSR, RCM, and motored engine conditions. Positive APCI was used to ionize isomers; the signals correspond to $C_8H_{15}O_3^+$ ions (*m/z* 159.1015).

These diketo-ethers, $C_8H_{14}O_3$, can oxidize and form olefinic diketo-ethers ($C_8H_{12}O_3$): O=Q=O + X$^{\bullet}$→ Q''(=O)$_2$+ XH; Q''(=O)$_2$ + O_2 → $^{\bullet}$OOQ'(=O)$_2$→ HOOQ''(=O)$_2$ (H-shift) → Q$^{''}$(=O)$_2$+ $HO_2^{\bullet}$. Using UHPLC-APCI(+)-HRMS, signals of $C_8H_{13}O_3^+$ ions (*m/z* 157.0858) were detected in samples obtained using the three experimental setups. As can be seen from Figure 10, several $C_8H_{13}O_3^+$ isomers are present in all the samples. For example, at R_t = 6.62 for JSR, RCM, and motored engine, at R_t = 7.05 min for JSR and motored engine, and at R_t = 9.09 min for JSR and RCM. However, one can note that the JSR sample, more concentrated, allowed the detection of more isomers.

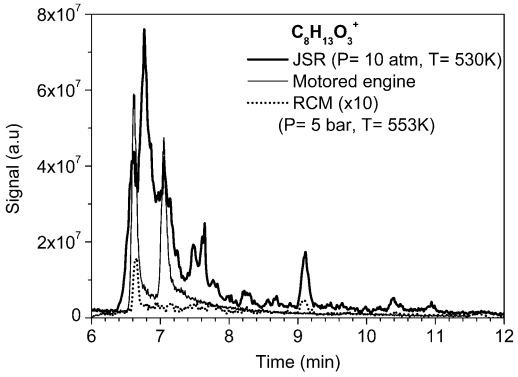

Figure 10. Comparison of chromatograms obtained in C_{18}-UHPLC-APCI (+)-HRMS analyses of JSR, RCM, and motored engine samples. The signal of $C_8H_{13}O_3^+$ (*m/z* 157.0858) ions is plotted.

The chemical formulae $C_8H_{12}O_3$ can also correspond to tri-olefinic hydroperoxides, although their formation is not considered in combustion schemes. Nevertheless, we tried to distinguish between the olefinic diketones and tri-olefinic hydroperoxides. As mentioned previously, DNPH derivatization allows to characterize the isomers having carbonyl function. The comparison between the $C_8H_{13}O_3^+$ chromatograms recorded before and after DNPH derivatization (Figure 11) allowed identifying the peaks corresponding to isomers that did not react with DNPH (tri-olefinic hydroperoxides). On can note that peaks at R_t of 6.62, 7.59, and R_t >10 min, have totally reacted with DNPH. Isomers at Rt = 7.05 min, and 7.60 <R_t< 9.88 min, have partially reacted. These observations indicate a preferential reactivity

of the olefinic diketo-ethers isomers with DNPH. According the position of the ketone functions, the reaction with DNPH can be influenced. For example, two adjacent ketone functions can create steric hindrance, limiting the reaction with DNPH. However, it seems that isomers observed at R_t of 6.76 and 7.20 min did not react with DNPH. This can indicate that these species might correspond to tri-olefinic hydroperoxides or other isomers without a carbonyl function. The relatively strong signal observed was unexpected.

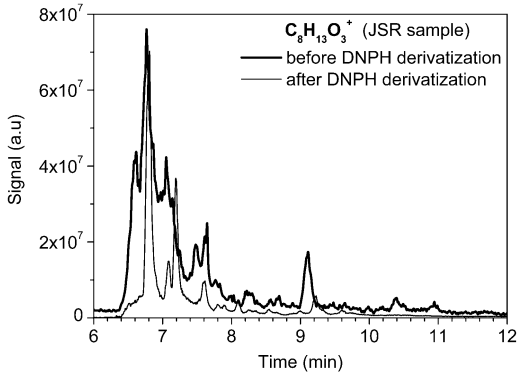

Figure 11. Chromatograms obtained by UHPLC-APCI(+)-HRMS. The signals of $C_8H_{13}O_3^+$ ions (*m/z* 157.0858) recorded before and after DNPH derivatization are presented.

3.5 Formation of keto-dihydroperoxides ($C_8H_{16}O_6$). Highly oxygenated chemicals such as keto-dihydroperoxides, $C_8H_{16}O_6$, resulting from a third O_2 addition on fuel's radicals are formed via the following reaction pathway: fuel + X$^\bullet$ ($^\bullet$OH, H$^\bullet$, O$^\bullet$, $HO_2^\bullet$, O_2…) → R$^\bullet$ + XH; R$^\bullet$ + O_2 → ROO$^\bullet$ → $^\bullet$QOOH (H-shift); $^\bullet$QOOH + O_2 → $^\bullet$OOQOOH → HOO$^\bullet$Q'OOH (H-shift); HOO$^\bullet$Q'OOH + O_2 → $(HOO)_2$Q'OO$^\bullet$ → $(HOO)_2$Q''=O + $^\bullet$OH. UHPLC-HRMS (APCI–) analyses of samples obtained under JSR and motored engine conditions showed the presence of several $C_8H_{16}O_6$ isomers ($C_8H_{15}O_6^-$, *m/z* 207.0875). As can be seen from Figure 12, the number of $C_8H_{15}O_6^-$ isomers detected in JSR samples is significantly higher (~ thirty peaks) than in motored engine samples (~ ten peaks). Several explanations can be offered to rationalize this result. Among them, a lower formation of $C_8H_{16}O_6$ species in the motored engine could be due to shorter reaction time and decomposition on exhaust metallic surfaces. To further assess the presence of these species in the engine samples, we performed H/D exchange followed by FIA-APCI(–)- HRMS. The results are presented in Table 3. One can note the formation of $C_8H_{13}D_2O_6^-$ ions corresponding to a keto-dihydroperoxide.

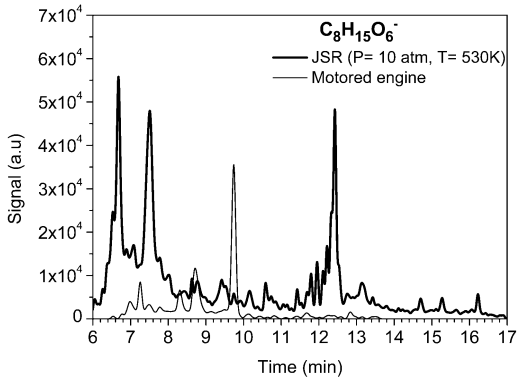

Figure 12. Comparison between C_{18}-UHPLC-HRMS (APCI-) signal for $C_8H_{15}O_6^-$ (*m/z* 207.0875) corresponding to keto-dihydroperoxide isomers formed in JSR and motored engine conditions.

3.6 Formation of diketo-hydroperoxides ($C_8H_{14}O_5$). The oxidation of keto-dihydroperoxides ($C_8H_{16}O_6$) can produce diketo-hydroperoxides species ($C_8H_{14}O_5$): $(HOO)_2Q''=O + X^{\bullet} \rightarrow (HOO)Q''=(O)_2 + XH + {}^{\bullet}OH$. UHPLC-APCI(–)-HRMS analyses revealed the presence of several $C_8H_{13}O_5^-$ (*m/z* 141.0924) isomers, in both JSR and motored engine samples. However, no signal was detected in the less concentrated RCM sample. As shown in Figure 13, more $C_8H_{13}O_5^-$ isomers are present in the JSR sample. Most of the chromatographic peaks with $R_t < 9$ min are present in both samples. Peaks with $R_t > 9$ min, already corresponding to minor products under the JSR conditions, are not observed in the motored engine sample.

One could observe a less important formation of diketo-hydroperoxides isomers in the engine, which is consistent with the less important formation of keto-dihydroperoxides ($C_8H_{16}O_6$) from which they derive (see Section 3.5).

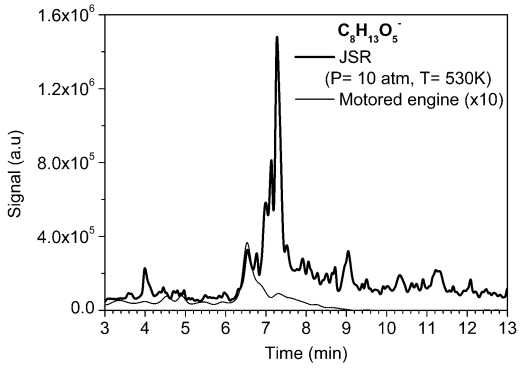

Figure 13. Comparison of chromatograms obtained by C_{18}-UHPLC-APCI(–)-HRMS analyses. Signals of $C_8H_{13}O_5^-$ (*m/z* 189.0165) ions correspond to diketo-hydroperoxides isomers formed in JSR and motored engine experiments.

3.7 Formation of lower mass carbonyls and carboxylic acids. Besides the aforementioned oxidation products detected in motored engine exhaust samples, more common unburnt species already reported in the literature[29-30] were detected using 2,4-dinitrophenyl hydrazine derivatization (Supporting

Information 2, Table S1). The following species were detected based on injection of pure standards: formaldehyde, acetaldehyde, propanal, acetone, acrolein, methacrolein, crotonaldehyde, methyl vinyl ketone (MVK), butanal, 2-butanone, formic acid, acetic acid, propanoic acid, and butyric acid.

3.8 Formation of hydroxy-DBE ($C_8H_{18}O_2$) and ROOR′ ($C_{16}H_{34}O_4$, $C_{11}H_{24}O_3$, $C_{11}H_{22}O_3$, and $C_{10}H_{22}O_3$). As mentioned in our previous work[28], other reaction routes, besides those usually considered in combustion models, can occur during the cool flame oxidation of fuels, i.e, 2 ROO$^{\bullet}$ → ROOOOR → 2 RO$^{\bullet}$ + O_2; RO$^{\bullet}$→ $^{\bullet}$QOH (H-shift); $^{\bullet}$QOH + O_2 → $^{\bullet}$OOQOH → OQ'OH + $^{\bullet}$OH; ROO$^{\bullet}$+ R'OO$^{\bullet}$ → ROOR' + O_2; ROO$^{\bullet}$+ R'OO$^{\bullet}$ → ROH + R'$_{(-H)}$=O + O_2. Although these oxidation channels are more representative of atmospheric chemistry, ROOR' and ROH were observed in JSR, RCM, and motored engine samples. APCI(+)-HRMS analyses allow detecting $C_8H_{18}O_2$ species corresponding to hydroxy-DBE (Figure 14) and organic peroxides: $C_{16}H_{34}O_4$ (with R=R'= $C_8H_{17}O$), $C_{11}H_{24}O_3$ (with R= $C_8H_{17}O$ and R'= C_3H_7), $C_{11}H_{22}O_3$ (with R= $C_8H_{15}O$ and R'= C_3H_7), and $C_{10}H_{22}O_3$ (with R= $C_8H_{17}O$ and R'= C_2H_5). The results obtained for ROOR' are shown in Table 4. One can note that as for the majority of the other oxygenated intermediates formed under JSR, RCM, and motored engine conditions, the ROOR' are better detected in the JSR samples (JSR > motored engine > RCM). UHPLC-HRMS analyses revealed that several $C_8H_{18}O_2$ isomers are present in the exhausts. Chromatograms of $C_8H_{19}O_2^+$ (*m/z* 147.1378) are presented in Figure 14. Four species were detected, which seems to indicate that all the possible hydroxy-DBE isomers are formed (JSR > motored engine > RCM). Based on MS/MS analyses on could identify that the pic at Rt = 8.9 min corresponds to $C_4H_9OCH(OH)C_3H_7$ ($C_5H_{11}O$+ fragment is not formed) and that the pic at Rt = 9.1 min corresponds to $C_4H_9OCH_2CH(OH)C_2H_5$ ($C_5H_{11}O$+ is the main fragment), see Table 5.

Table 4. Comparison between HRMS signals of ROOR' from JSR (530 K), RCM (553 K), and motored engine samples analyzed by FIA.

Sample	$C_{16}H_{34}O_4$ *m/z* $(M+H)^+$ 291.2528	$C_{11}H_{24}O_3$ *m/z* $(M+H)^+$ 205.1797	$C_{11}H_{22}O_3$ *m/z* $(M+H)^+$ 203.1640	$C_{10}H_{22}O_3$ *m/z* $(M+H)^+$ 191.1641
JSR	2.35×10^6	1.91×10^6	1.59×10^6	1.24×10^6
RCM	1.25×10^5	1.68×10^5	1.79×10^4	1.99×10^4
Motored engine	4.22×10^5	4.67×10^5	1.34×10^5	5.39×10^4

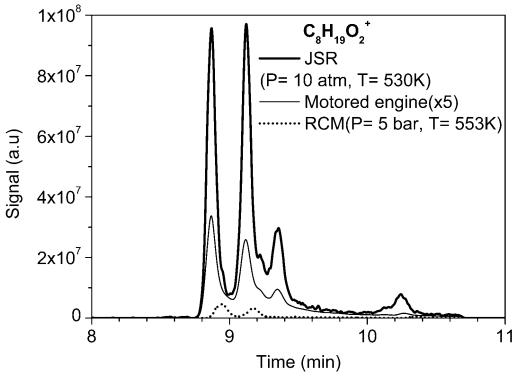

Figure 14. Comparison of chromatograms obtained by C_{18}-UHPLC-APCI(+)-HRMS analyses of JSR, RCM, and motored engine samples. The signals for $C_8H_{19}O_2^+$ (*m/z* 147.1378) correspond to hydroxy-DBE isomers formed under three experimental conditions.

Table 5. MS/MS analyzes of ROH ($C_8H_{19}O_2^+$)

ROH isomers ($C_8H_{19}O_2^+$, *m/z* 147.1378)	$C_8H_{17}O^+$ *m/z* 129.1270 $C_8H_{19}O_2^+ - H_2O$	$C_5H_{11}O^+$ *m/z* 87.0809 $C_8H_{17}O^+ - C_3H_6$	$C_4H_9O^+$ *m/z* 73.0654 $C_8H_{17}O^+ - C_4H_8$	$C_4H_9^+$ *m/z* 57.0696 $C_8H_{17}O^+ - C_4H_8O$
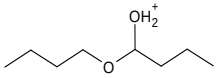 Rt = 8.90 min	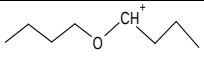	-	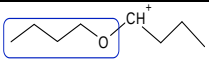	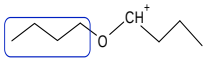
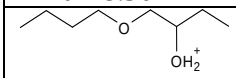 Rt = 9.10 min	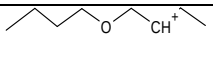	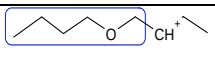	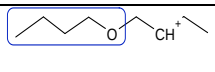	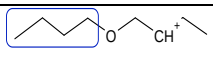
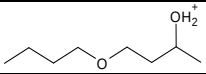	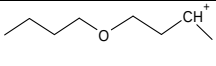	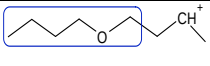	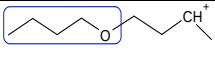	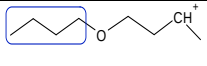
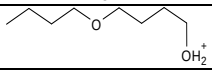	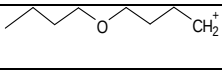	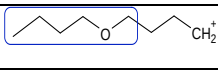	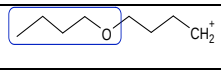	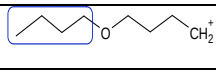

4. CONCLUSIONS

The cool flame oxidation of di-*n*-butyl ether/air mixtures was investigated in a modified single-cylinder Diesel engine running in HCCI mode. The engine was coupled to an electric motor to operate at constant rotation speed. The exhaust gases were collected using a bubbler containing cooled acetonitrile. Low-temperature oxidation intermediates and products were detected using liquid chromatography coupled to high resolution mass spectrometry and APCI (+/–). These species include diols and hydroperoxides ($C_8H_{18}O_3$), unsaturated diols, hydroperoxides ($C_8H_{16}O_3$), ketohydroperoxides ($C_4H_8O_3$ and $C_8H_{16}O_4$), diketo-ethers ($C_8H_{14}O_3$), olefinic di-keto ethers ($C_8H_{12}O_3$), cyclic ethers or keto-ethers ($C_8H_{16}O_2$), olefinic cyclic and keto-ethers ($C_8H_{14}O_2$), hydroxy-DBE ($C_8H_{18}O_2$), highly oxygenated chemicals, i.e., keto-dihydroperoxides ($C_8H_{16}O_6$) and diketo-hydroperoxides ($C_8H_{14}O_5$). In addition, signals corresponding to organic peroxides ROOR' ($C_{16}H_{34}O_4$, $C_{11}H_{24}O_3$, $C_{11}H_{22}O_3$, and $C_{10}H_{22}O_3$), were detected in JSR, RCM, and motored engine samples. To assess the presence of OH

and OOH groups in products, we performed H/D exchange using D_2O and flow injection analyzes coupled to APCI (+/–) and HRMS. This procedure was particularly useful for confirming the presence of ROOH, diols, unsaturated ROOH and diols, keto-dihydroperoxides, diketohydroperoxides and hydroxy-DBE. Chromatographic analyzes of motored engine, JSR, and RCM samples were performed. The comparison of the results showed impressive similarities, although variable proportions of products were observed, which could be due to concentrations in samples, decomposition of less stable products on metallic surfaces (RCM, engine), different reaction temperature. This result implies that similar chemical processes take place in the three experimental systems selected for this study (JSR, RCM, and motored engine), despite their rather different physical conditions (temperature, pressure, reaction time, initial reactant concentrations. Also, the present study demonstrates that besides carbon dioxide and volatile organic compounds (unburnt hydrocarbons, aldehydes, ketones, carboxylic acids, ketohydroperoxides, cyclic ethers …) other organic compounds produced in cool flames, and never reported before, can be present in exhausts engines fueled with DBE, i.e., hydroperoxides and diols, unsaturated diols or hydroperoxides, di-keto ethers, olefinic di-keto ethers, keto-ethers, olefinic cyclic ethers and keto-ethers, and highly oxygenated chemicals (keto-dihydroperoxides and diketo-hydroperoxides). This work also demonstrates the usefulness of chromatographic analyses to characterizing isomeric products. The formation and consumption reactions of all these species should be considered in proposed kinetic models; this could help improving simulations of fuels ignition and get better prediction of piston engines emissions.

■ ASSOCIATED CONTENT

Supporting information: **(1)** MS/MS data for hydroperoxides and diols, **(2) Table S1** Identification of carbonyl compounds through 2,4-DNPH derivatization.

■ ACKNOWLEDGEMENTS

The authors acknowledge financial support from the Labex CAPRYSSES (convention ANR-11-LABX-0006-01) and from the Region Centre Val de Loire, European Funds for Regional Development, and CPER (projects PROMESTOCK and APROPOR-E).

AUTHORS

Nesrine Belhadj − Institut de Combustion, Aérothermique, Réactivité et Environnement (ICARE), Centre National de la Recherche Scientifique (CNRS), 45071 Orléans, France; Université d'Orléans, 45067 Orléans, France ORCID: 0000-0002-5860-4144

Maxence Lailliau − Institut de Combustion, Aérothermique, Réactivité et Environnement (ICARE), Centre National de la Recherche Scientifique (CNRS), 45071 Orléans, France; Université d'Orléans, 45067 Orléans, France ORCID: 0000-0002-7758-3756

Zahraa Dbouk− Institut de Combustion, Aérothermique, Réactivité et Environnement (ICARE), Centre National de la Recherche Scientifique (CNRS), 45071 Orléans, France; Université d'Orléans, 45067 Orléans, France. ORCID: 0000-0002-8797-2990

Roland Benoit − Institut de Combustion, Aérothermique, Réactivité et Environnement (ICARE), Centre National de la Recherche Scientifique (CNRS), 45071 Orléans, France. ORCID: 0000-0001-8898-6131

Bruno Moreau – Laboratoire PRISME, Université d'Orléans, 45067 Orléans, France. ORCID: 0000-0002-6240-1710

Fabrice Foucher – Laboratoire PRISME, Université d'Orléans, 45067 Orléans, France. ORCID: 0000-0001-8469-8546

Philippe Dagaut − Institut de Combustion, Aérothermique, Réactivité et Environnement (ICARE), Centre National de la Recherche Scientifique (CNRS), 45071 Orléans, France. ORCID: 0000-0003-4825-3288

■ REFERENCES

(1) Affleck, W. S.; Fish, A., Two-stage ignition under engine conditions parallels that at low pressures. *Symposium (International) on Combustion* **1967,** *11* (1), 1003-1013.

(2) Leppard, W. R., The Autoignition Chemistry of n-Butane: An Experimental Study. *SAE Tech. Pap.* **1987**, 872150.

(3) Leppard, W. R., The Autoignition Chemistry of Isobutane: A Motored Engine Study. *SAE Tech. Pap.* **1988**, 881606.

(4) Leppard, W. R., A Comparison of Olefin and Paraffin Autoignition chemistries: A Motored-Engine Study. *SAE Tech. Pap.* **1989**, 892081.

(5) Sahetchian, K.; Champoussin, J. C.; Brun, M.; Levy, N.; Blin-Simiand, N.; Aligrot, C.; Jorand, F.; Socoliuc, M.; Heiss, A.; Guerassi, N., Experimental study and modeling of dodecane ignition in a diesel engine. *Combust. Flame* **1995,** *103* (3), 207-220.

(6) Blin-Simiand, N.; Jorand, F.; Keller, K.; Fiderer, M.; Sahetchian, K., Ketohydroperoxides and ignition delay in internal combustion engines. *Combust. Flame* **1998,** *112*, 278-282.

(7) Blin-Simiand, N.; Jorand, F.; Sahetchian, K.; Brun, M.; Kerhoas, L.; Malosse, C.; Einhorn, J., Hydroperoxides with zero, one, two or more carbonyl groups formed during the oxidation of n-dodecane. *Combust. Flame* **2001,** *126* (1), 1524-1532.

(8) Wang, Z. D.; Chen, B. J.; Moshammer, K.; Popolan-Vaida, D. M.; Sioud, S.; Shankar, V. S. B.; Vuilleumier, D.; Tao, T.; Ruwe, L.; Brauer, E., et al., n-Heptane cool flame chemistry: Unraveling intermediate species measured in a stirred reactor and motored engine. *Combust. Flame* **2018,** *187*, 199-216.

(9) Szybist, J. P.; Boehman, A. L.; Haworth, D. C.; Koga, H., Premixed ignition behavior of alternative diesel fuel-relevant compounds in a motored engine experiment. *Combust. Flame* **2007,** *149* (1-2), 112-128.

(10) Yang, Y.; Boehman, A. L., Experimental study of cyclohexane and methylcyclohexane oxidation at low to intermediate temperature in a motored engine. *Proc. Combust. Inst.* **2009,** *32* (1), 419-426.

(11) Zhang, Y.; Boehman, A. L., Experimental study of the autoignition of C8H16O2 ethyl and methyl esters in a motored engine. *Combust. Flame* **2010,** *157* (3), 546-555.

(12) Zhang, Y.; Boehman, A. L., Oxidation of 1-butanol and a mixture of n-heptane/1-butanol in a motored engine. *Combust. Flame* **2010,** *157* (10), 1816-1824.

(13) Liu, H.; Yao, M.; Zhang, B.; Zheng, Z., Effects of Inlet Pressure and Octane Numbers on Combustion and Emissions of a Homogeneous Charge Compression Ignition (HCCI) Engine. *Energy Fuels* **2008,** *22* (4), 2207-2215.

(14) Mofijur, M.; Hasan, M. M.; Mahlia, T. M. I.; Rahman, S. M. A.; Silitonga, A. S.; Ong, H. C., Performance and Emission Parameters of Homogeneous Charge Compression Ignition (HCCI) Engine: A Review. *Energies* **2019,** *12* (18), 3557.

(15) Al-Gharibeh, E.; Beyerlein, S.; Kumar, K., Speciation and Heat Release Studies during n-Heptane Oxidation in a Motored Engine. *Combust. Sci. Technol.* **2021**, 1-25.

(16) Al-Gharibeh, E.; Kumar, K., Oxidation kinetics of methyl decanoate in a motored engine. *Fuel* **2022,** *308*, 121912.

(17) Belhadj, N.; Lailliau, M.; Dbouk, Z.; Benoit, R.; Moreau, B.; Foucher, F.; Dagaut, P., Gasoline surrogate oxidation in a motored engine, a JSR, and an RCM: Characterization of cool-flame products by high-resolution mass spectrometry. *Energy Fuels* **2022,** *36* (7), 3893–3908.

(18) Belhadj, N.; Benoit, R.; Dagaut, P.; Lailliau, M.; Moreau, B.; Foucher, F., Low-temperature oxidation of a gasoline surrogate: Experimental investigation in JSR and RCM using high-resolution mass spectrometry. *Combust. Flame* **2021,** *228*, 128-141.

(19) Belhadj, N.; Benoit, R.; Dagaut, P.; Lailliau, M.; Serinyel, Z.; Dayma, G.; Khaled, F.; Moreau, B.; Foucher, F., Oxidation of di-n-butyl ether: Experimental characterization of low-temperature products in JSR and RCM. *Combust. Flame* **2020,** *222*, 133-144.

(20) Dagaut, P.; Cathonnet, M.; Rouan, J. P.; Foulatier, R.; Quilgars, A.; Boettner, J. C.; Gaillard, F.; James, H., A jet-stirred reactor for kinetic studies of homogeneous gas-phase reactions at pressures up to ten atmospheres (~ 1 MPa). *Journal of Physics E-Scientific Instruments* **1986,** *19* (3), 207-209.

(21) Pochet, M.; Dias, V.; Moreau, B.; Foucher, F.; Jeanmart, H.; Contino, F., Experimental and numerical study, under LTC conditions, of ammonia ignition delay with and without hydrogen addition. *Proc. Combust. Inst.* **2019,** *37* (1), 621-629.

(22) Belhadj, N.; Benoit, R.; Dagaut, P.; Lailliau, M., Experimental characterization of n-heptane low-temperature oxidation products including keto-hydroperoxides and highly oxygenated organic molecules (HOMs). *Combust. Flame* **2021,** *224*, 83-93.
(23) Belhadj, N.; Lailliau, M.; Benoit, R.; Dagaut, P., Experimental and kinetic modeling study of n-pentane oxidation at 10 atm, Detection of complex low-temperature products by Q-Exactive Orbitrap. *Combust. Flame* **2022,** *235*, 11723-11723.
(24) Sattler, A., Hydrogen/Deuterium (H/D) Exchange Catalysis in Alkanes. *ACS Catalysis* **2018,** *8* (3), 2296-2312.
(25) Belhadj, N.; Benoit, R.; Dagaut, P.; Lailliau, M.; Serinyel, Z.; Dayma, G., Oxidation of di-n-propyl ether: Characterization of low-temperature products. *Proc. Combust. Inst.* **2021,** *38* (1), 337-344.
(26) Belhadj, N.; Benoit, R.; Dagaut, P.; Lailliau, M., Experimental Characterization of Tetrahydrofuran Low-Temperature Oxidation Products Including Ketohydroperoxides and Highly Oxygenated Molecules. *Energy Fuels* **2021,** *35* (9), 7242–7252.
(27) Jensen, R. K.; Korcek, S.; Mahoney, L. R.; Zinbo, M., Liquid-phase autoxidation of organic-compounds at elevated-temperatures .1. stirred flow reactor technique and analysis of primary products from normal-hexadecane autoxidation at 120-degrees-C 180-degrees-C. *J. Am. Chem. Soc.* **1979,** *101* (25), 7574-7584.
(28) Belhadj, N.; Lailliau, M.; Benoit, R.; Dagaut, P., Towards a Comprehensive Characterization of the Low-Temperature Autoxidation of Di-n-Butyl Ether. *Molecules* **2021,** *26* (23), 7174.
(29) Tran, L. S.; Wullenkord, J.; Li, Y. Y.; Herbinet, O.; Zeng, M. R.; Qi, F.; Kohse-Hoinghaus, K.; Battin-Leclerc, F., Probing the low-temperature chemistry of di-n-butyl ether: Detection of previously unobserved intermediates. *Combust. Flame* **2019,** *210*, 9-24.
(30) Thion, S.; Togbe, C.; Serinyel, Z.; Dayma, G.; Dagaut, P., A chemical kinetic study of the oxidation of dibutyl-ether in a jet-stirred reactor. *Combust. Flame* **2017,** *185*, 4-15.
(31) Pelucchi, M.; Bissoli, M.; Cavallotti, C.; Cuoci, A.; Faravelli, T.; Frassoldati, A.; Ranzi, E.; Stagni, A., Improved Kinetic Model of the Low-Temperature Oxidation of n-Heptane. *Energy Fuels* **2014,** *28* (11), 7178-7193.